

Block Copolymer Assemblies as Templates for the Generation of Mesoporous Inorganic Materials and Crystalline Films

Bernd Smarsly^[a] and Markus Antonietti*^[a]

Keywords: Block copolymers / Mesoporous materials / Self-assembly / Sol–gel processes

This Microreview presents the synthesis of mesoporous, crystalline inorganic materials using self-assembled block copolymer mesostructures as templates. The advances in this field are discussed in light of the progress in the development of suitable polymer templates. Particular emphasis is placed on

the special conditions and demands to transform the primary sol–gel films into mesoporous, aligned crystalline films for functional applications.

(© Wiley-VCH Verlag GmbH & Co. KGaA, 69451 Weinheim, Germany, 2006)

Introduction

In the past ten years scientists have learned to develop and use appropriate amphiphilic block copolymers (soft matter) as templates to generate inorganic films and multocrystals with controlled porosity on the nanometer scale (hard matter). Such inorganic materials with a nanoscale structural set-up and large specific surfaces had not been accessible before and may play important roles in sorption, catalysis, photoconversion, or piezo- and ferroelectric devices.

This Microreview will introduce the concept of “true liquid-crystal templating”,^[1,2] i.e. the idea of converting a self-assembled block copolymer mesophase into its inorganic counterpart with liquid precursors (e.g. providing mesoporous silica, metal oxides, and metals), which is also termed “nanocasting”.^[3] We will delineate the special effects for a number of oxide crystalline systems with special functions in detail.

The field of mesoporous oxides made by templates is, of course, much bigger, and for a general overview of ordered mesoporous oxides we refer the reader to the review article by Schüth.^[4] This review will be centered around the generation of mesoporous inorganic structures using block copolymers as templates, putting special emphasis on the con-

[a] Max-Planck Institute of Colloids and Interfaces, Am Mühlenberg, 14476 Potsdam-Golm, Germany



Bernd Smarsly studied chemistry and physics at the University of Marburg, Germany, and Innsbruck, Austria, and received a Masters degree of Natural Science in 1998. He completed his PhD studies in 2001 at the Max Planck Institute of Colloids and Interfaces. Afterwards, from 2002–2003 he worked as a postdoctoral researcher at the Advanced Materials Laboratory of the University of New Mexico at Albuquerque, USA. Since 2003 he has been working as group leader at the MPI of Colloids and Interfaces. His main research interests now focus on the preparation of functional, mesostructured metal oxides, their physico-chemical properties, and the development of novel characterization techniques, especially using X-ray scattering.



Markus Antonietti studied chemistry in Mainz and did his doctorate with Hans Sillescu. His habilitation about nanostructured polymer gels in 1990 filled him with enthusiasm for complex materials. After his Professorship of Chemistry at the University of Marburg, he was appointed Director of the Department of Colloid Chemistry at the Max Planck Institute of Colloids and Interfaces in 1993. Markus Antonietti's contributions to the chemical community are manifold, but first of all he is interested in the creativity in research. He loves to share and impart this passion. He also likes cooking with his family and loud music.

MICROREVIEWS: This feature introduces the readers to the authors' research through a concise overview of the selected topic. Reference to important work from others in the field is included.

ditions of crystalline metal-oxide formation and the observed textural properties. While most of the research is focused on oxide materials, a separate paragraph is reserved for the interesting emerging field of mesoporous metals.

1. General Mechanism

The general idea of using block copolymers as templates is based on the fact that amphiphilic block copolymers self-assemble in certain solvents to give robust, very regular superstructures that feature structural motifs on the nanometer scale (lyotropic liquid-crystalline phases). Typically, the constituting entities are spherical or cylindrical micelles or lamellar sheets with a characteristic cross-section of 5–100 nm.

The block copolymer self-assembly technique is probably the best examined mode of self-organization^[5] and is governed by the microphase separation dictated by the mutual incompatibility of the different blocks, one being soluble and the other being insoluble in the solvent to be used (“amphiphilic” polymers). In most cases, aside from classical nonionic surfactants, which can be regarded as small block oligomers composed of an oligoethylene and oligo(ethylene oxide), diblock or triblock copolymers are used that feature polystyrene,^[2a] polybutadiene,^[6] and poly(propylene oxide) as the hydrophobic block,^[7] and poly(ethylene oxide) or poly(vinylpyridines)^[8] as hydrophilic blocks. Recently, a semi-commercial family of “KLE” block copolymers [KLE = *Kraton-Liquid-b-poly(ethylene oxide)*] was introduced, which combines good chemical accessibility and high mesophase robustness with a superb application profile.^[9] Kraton liquid is a hydrogenated poly(ethylene-*co*-butylene) hydrophobic block with a low glass transition. In principle, block copolymers self-assemble or microphase-separate in a variety of solvents, in particular water, but also alcohols or THF, which enables a certain width of chemistry for inorganic framework generation. This is contrary to low molecular weight surfactants, which usually rely on water and the hydrophobic effect for self-assembly.

In a typical block copolymer templating procedure (see Figure 1), such regularly ordered mesostructures of amphiphiles in water are converted into their 1:1 replica (their “negative”) by solidifying the hydrophilic or solvatophilic domains between the micelles. This is done by replacing the majority of the solvent by a metal or metal oxide precursor with similar polarity and condensing this precursor around

the aggregates. An especially suitable precursor for this procedure is, for instance, hydrated silicic acid, which shows a very similar polarity and proton-bridging behavior as water, such that the final assembly patterns are very similar to the ones found in water. Depending on the final material of choice, this precursor can be a hydrolysable metal species such as metal-orthoesters, but can also be a metal salt (metal chlorides, etc.), and the final structure can be made out of metal oxides, metal chalcogenides, or even the elemental metals. The organic template can also be regarded as a place holder that prevents the inorganic reaction from occurring and becomes void space upon removal either by extraction or thermal decomposition.

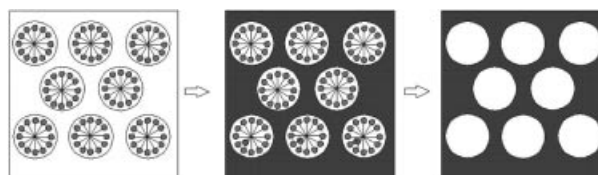


Figure 1. Illustration of the typical block copolymer templating procedure (“nanocasting”). A soft matter complex fluid is surrounded with a high concentration of inorganic precursor (left), and the continuous phase is solidified (middle). After solidification of the inorganic phase, the template is removed to give a solid negative replica (“hardcopy”) of the original phase.

Figures 2 and 3 show examples of mesostructures that can be obtained by varying the polymers.^[6b]

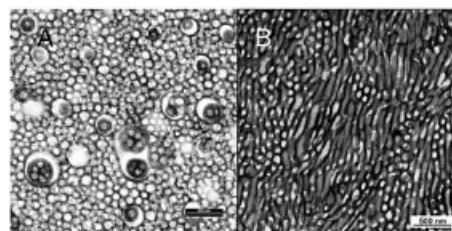


Figure 3. TEM of two mesoporous silicas obtained from PB-*b*-PEO templates,^[6] illustrating the wide range of accessible structures. **A** presents a micellar phase at the borderline to a lamellar phase, which contains some vesicles as precursor structures (scale bar: 200 nm), while **B** shows the bicontinuous sponge-like L_3 -phase (scale bar: 500 nm).

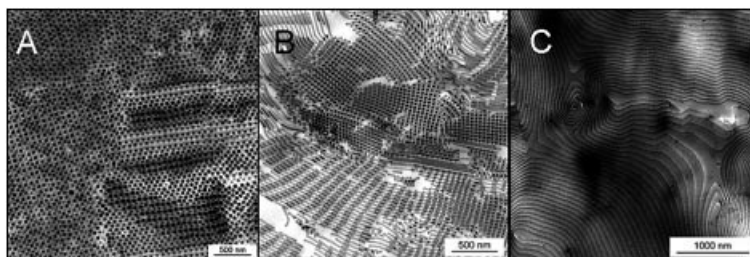


Figure 2. Microtomed films of lyotropic phases of block copolymers, as used for nanocasting. **A**: BCC phase; **B**: hexagonal phase; **C**: lamellar phase (taken from refs.^[6b,6c]).

bic, etc.) and a wider range of accessible pore sizes, currently up to about 80 nm.^[6] Initial work was pioneered by Göltner et al. using PS-*b*-PEO^[2] or PS-*b*-PVP block copolymers.^[8] Later, presumably independently, this work was extended by Stucky towards Pluronics block copolymers^[7] and by Wiesner et al.^[10] towards organically modified aluminosilica hybrids.

The assumption that the final silica mesostructure represents a 1:1 copy of the lyotropic phase was later proven by comparing the replicas with species obtained by cross-linking of lyotropic phases with γ -radiation.^[11] An unusual case is shown in Figure 4, where a branched lamellar phase is replicated and compared with the original phase. The two TEM images show the original lyotropic phase (Figure 4, A) and the templated, porous silica (Figure 4, B), and it is nicely seen that one is the “negative” of the other.

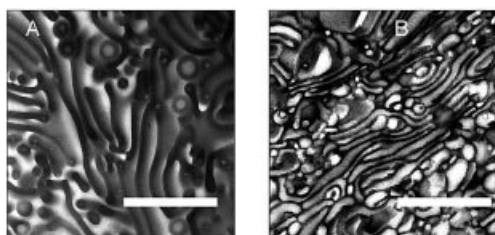


Figure 4. Original or copy? A represents the lyotropic phase (TEM obtained from thin cuts) leading to the corresponding silica (B) shown in Figure 3. This example illustrates the similarity between the original block copolymer mesophase and the silica replica. Terminal ends of lamellae, branching points, vesicles, membrane, and pores are replicated with about the same abundance and fine structural features. The scale bars represent 1000 nm.

The quality of replication plus the homogeneity has also been proved by small angle X-ray scattering. Already in the original paper by Göltner et al.^[2c] the authors showed that after solidification and removal of the template the diffractogram is only shifted to slightly higher angles, while the pattern stays unaltered. This means that the material shrinks slightly but does not change its local structure. A case for quantitative fitting of the scattering curve is shown in Figure 5.

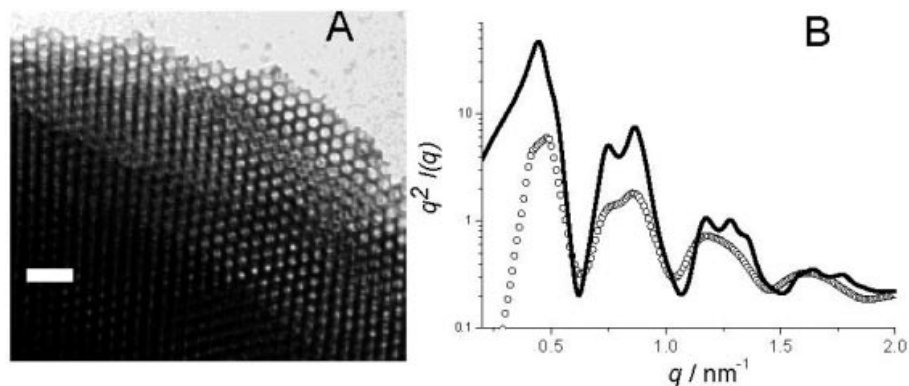


Figure 5. Mesoporous silica featuring spherical mesopores (size of about 13 nm) obtained from the KLE block copolymer [poly(ethylene-co-butylene)-*b*-poly(ethylene oxide)].^[9a] The TEM image (A) reveals a highly ordered structure of spherical mesopores arranged on a fcc lattice. The scale bar is 80 nm. B: Small-angle X-ray scattering curve of the mesoporous silica (circles) and a fitting (solid line) based on a model of spherical mesopores with a certain polydispersity and lattice distortions^[9a] In the present case, the relative polydispersity of the pore radius is only 5% (including the deviations from spherical shape).

In this case (using KLE polymers as a template), TEM shows that the mesoporous silica contains a regular packing of spherical mesopores about 13 nm in diameter, which are located on the sites of a face-centered cubic arrangement. Evidently, not only are the single mesopores extremely uniform in shape and size, but the 3D arrangement is also nearly undisturbed over large areas of up to several square micrometers. This example illustrates the amazing order and control of the materials' structure that can be achieved by the nanocasting procedure, in spite of the mechanical stresses during the condensation of the matrix. Small-angle X-ray scattering (SAXS) is usually applied to provide an overall, averaged characterization of mesoporous materials. In this case (Figure 5, b), the presence of distinct SAXS patterns with pronounced maxima and minima confirms the high regularity of the mesostructure and the mesopore size and lattice type.

In the case of metal oxides the ultimate composition is readily obtained by heat-treatment in air or oxygen to give the amorphous or crystalline oxide form, and mesoporous metals are obtained by an in situ or final reduction step, either electrochemically or chemically.

2. Evaporation-Induced Self-Assembly for the Generation of Organized Thin Films

The general concept of nanocasting was originally developed for thick specimens (monoliths or powders), although it also holds true for the generation of bulk materials and thin films. The latter was remarkably improved and simplified by introduction of the technique of “evaporation-induced self-assembly” (EISA).^[12] EISA proceeds along a different methodology, but the underlying templating mechanism is identical to nanocasting. The practical difference lies in the fact that one starts from a homogeneous solution with a significantly larger amount of volatile solvents with low viscosity.

Taking this low viscosity, which means less organized precursor solutions, coatings of excellent macroscopic

homogeneity can be generated by standard coating techniques, i.e. dip-coating, spin-coating, doctor-blading, or spraying. After evaporation of the volatile solvent, a high-concentration template phase is regained. This is the return to the situation of nanocasting, although already shaped in a defined coating geometry. It must be mentioned, however, that throughout drying, large scale orientation of the otherwise unorganized lyotropic phase can be promoted to a very high extent. For EISA in thin films, the strong interaction with the substrate in the interplay with a directional drying pressure (e.g. in dip coating) usually leads to a high degree of preferred orientation, much higher than in the bulk materials.^[13] An orientation is usually established that provides a maximum degree of interaction with the substrate via the densest lattice plane.^[14]

For the generation of inorganic materials discussed below, low molecular weight inorganic precursors or salts are usually taken. Recent papers, however, have shown that similar constructions can also be achieved by EISA using preformed inorganic nanoparticles of sizes of only a few nanometers for structure build-up, e.g. TiO_2 ^[15] or CeO_2 ,^[16] as illustrated in Figure 6.

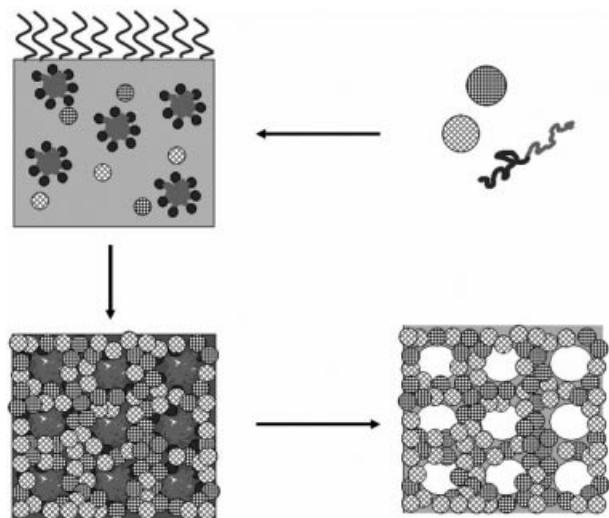


Figure 6. Block copolymer templating to generate a mesoporous scaffold starting from inorganic nanoparticles, using the EISA process. The scheme illustrates the more complicated case where two different nanoparticles ("bricks"), cross-hatched with vertical/horizontal and diagonal lines, respectively, are used for structure set-up to generate binary contacts.

It is evident that this approach faces different obstacles, for instance the colloidal stability of the initial sol, and only recently has a novel procedure for the synthesis of nanoparticles provided particles which could be sufficiently dispersed at high concentrations.^[17] On the other hand, there are also benefits due to the building block approach, as the material is already crystallized and does not shrink.^[16] Binary systems (i.e. two different nanoparticles) can also be easily made, thus leading to interesting binary contacts.

While the overall principle of block copolymer templating for inorganic chemistry seems to be surprisingly straightforward, it is worthwhile to highlight some key features of this process:

- Such high area interfaces between two materials can only be generated if all of the involved interfacial energies throughout the process are lowered. This compatibilization is provided by the special chemical character of the appropriate block copolymer. If a new inorganic substance is to be made porous, a block copolymer with the right binding moieties along the backbone of one block has to be chosen.

- As the formation of microphase-separated block copolymer phases is a thermodynamic phenomenon, templating is substantially governed by numerous physical parameters. Together with solvent effects, it is difficult to predict pore structures a priori, hence optimal templating conditions were found by trial-and-error experiments in many cases. In addition to these thermodynamic parameters, templating is further aggravated by strong kinetic effects, as some intermediary structures might turn out to be metastable. For instance, Gibaud et al. have shown that the rate of evaporation of the volatile solvent, even when all the other parameters are kept the same, can dramatically change the final mesophase structure.^[14]

- A general problem of true liquid-crystalline sol-gel templating is the simultaneous occurrence of condensation of the inorganic species and the self-assembly process. Experimental procedures are usually needed that delay the condensation significantly until completion of micelle formation. Robust self-assembly of amphiphilic copolymers into micelles, which is the best choice for systems with higher segregation strength (or incompatibility between the two blocks), is certainly favorable for this purpose. The use of block copolymers towards larger sizes is limited for the same reason by their increasingly reduced mobility. Hence, the upper limit for block copolymer templating is, under practical conditions, currently at about 80 nm in structural size.^[6]

- The solvating block is sometimes tightly bound and molecularly mixed into the inorganic phase, bringing some organic character to it, as found for PEO and silica.^[18] This can result, after template removal, in extensive extra microporosity (pore size below 2 nm), as reported by various studies.^[18–24] While physisorption techniques gave no unambiguous conclusion, detailed small-angle X-ray and neutron scattering (SAXS, SANS) analyses of PS-*b*-PEO-templated silicas provided a quantification of the microporosity^[21–23] and showed that the micropores are actually located between the mesopores.

3. Synthesis of Mesoporous, Crystalline Metal Oxides

While work in the first years of block copolymer templating has been mainly focused on amorphous silica as a model case, one of the current scientific challenges is the creation of mesoporous metal oxides whose pore walls are entirely nanocrystalline. The reason for this is essentially driven by their potential applications: crystalline oxides are chemically, thermally, and mechanically more robust. In addition, oxide materials possess inherently interesting func-

tionality, which is improved or is accessible by the introduction of mesopores. For instance, mesoporous, crystalline TiO_2 could be beneficial for various applications like solid-state solar cells ("the Grätzel cell")^[25] or photocatalysis.^[26] In these applications, organized porosity would be helpful to improve the contact between the oxide and other species (e.g. the anode in case of solar cells). Another target is heterogeneous catalysis, where it would be desirable to generate mesoporous metal oxides such as CeO_2 , ZrO_2 , or V_2O_5 .

The necessity of a high crystallinity imposes a severe problem. It is evident that the soft, self-assembled structures of amphiphilic block copolymers (ABC) are not very stable at the high temperatures needed for many crystallization processes of oxides. The use of preformed, soluble metal oxide nanoparticles for casting evidently has certain elegance because of the absence of a separate nucleation step for the oxide, but is still restricted to some readily dispersible oxides.^[16] This is why the most frequently employed strategy starts from molecular metal precursors such as metal chlorides or alkoxides (e.g. TiCl_4 , $\text{CeCl}_3 \cdot 7\text{H}_2\text{O}$, etc.). Many metal oxide precursors are indeed available that are amenable to sol-gel templating and are soluble in common solvents.

These precursors are then condensed, and nucleation and crystallization as well as the removal of the template occur concurrently and have to be dynamically balanced. This is not simple, as crystal growth can severely disrupt the fragile, soft ABC mesostructure, which would lead to pore collapse and loss of mesostructural order. Therefore, usually quite delicate and tedious heat-treatment procedures have to be used to avoid mesostructural breakdown and to balance condensation, crystallization, and calcination of the template.

Previous experiments with classical templates gave highly crystalline mesoporous oxides in only a few cases, in particular for TiO_2 .^[27–30] In the majority of these studies the materials showed either moderate crystallinity or significant damage to the mesostructural regularity (pore shape and porosity). A clever optimization of all these processes was presented by Grosso et al., who developed an in situ experiment to study the morphological changes by simultaneous small- and wide-angle X-ray scattering (SAXS/WAXS), leading to an improved understanding of the crystallization and its interference with the imprinted mesostructure.^[30c] Using that technique, crystalline mesoporous anatase became accessible with traditional templates.

Novel amphiphilic block copolymer templates helped to improve the preparation of mesoporous TiO_2 films^[31] and to extend these results also to other oxides of high chemical relevance. This is on the one hand due to the ability of these systems to self-assemble in a broader range of solvent systems: poly(ethylene-*co*-butylene)-*b*-poly(ethylene oxide) ("KLE polymers") is more robust and has more hydrophobic "contrast" than the commonly applied polymers of the Pluronics family.^[31b] Poly(isobutylene)-*b*-poly(ethylene oxide) (PIB-*b*-PEO)^[31a] is a similar template system with improved templating properties and good accessibility.

Secondly, due to their larger and chemically variable molecular weight, the pore structure can be adopted to match organic process parameters and properties, such as the nanocrystal size. If an inorganic system shows a small nucleation and fast growth-rate, the nanocrystals get rather big under standard conditions and the targeted pore size has to match the size of the accessible tectonic elements to form the structure. In other cases, the desired physical properties rely on a certain structural size, such as the excitation or plasmon size. Anatase just keeps its favorable indirect semiconductor properties at a size larger than 10 nm, and making the structure finer does not contribute to performance. For all those systems, the targeting of slightly larger pore sizes (ca. 20 nm) is advised.

Thirdly, the chemical functionality of the inorganic-binding block can also, in principle, be adjusted, for example by introduction of acetylacetoxy groups^[32] or a variety of other metal-complexing moieties, following the hard-soft-acid-base (HSAB) principle.^[33] Up to now, however, it has been possible to address all practical questions with the simple PEO binding block.

The final crystalline films are very homogeneous, crack-free, and flat on the scale of some nanometers over macroscopic dimensions. This is nicely illustrated by high resolution SEM of the surface of such an optimized anatase film (Figure 7). The depicted pores have a size of about 13 nm, are open to the surface, and at some positions even the three openings towards the lower cubic pore layer are visible. The overall flatness of this film (excluding pores) is lower than 2 nm, as determined by atomic force microscopy (AFM). It should be emphasized that these films show a rather homogeneous spherical pore shape. The structure resembles highly ordered inverse opal structures with respect to the perfection of the mutual arrangement, thus proving that crystal-like packing can also be achieved with block copolymers.

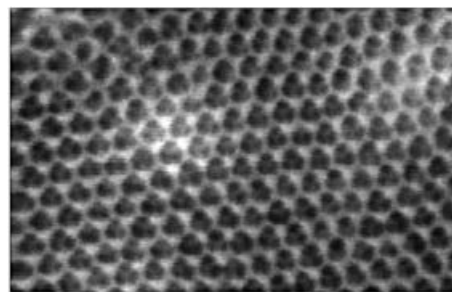


Figure 7. HRSEM of a mesoporous crystalline anatase film indicating the typical lyotropic liquid-crystalline arrangement of pores. The pores have a cross-section of about 13 nm. Note that in some pores the three entries to the lower layer of the cubically packed pores are visible.

With these improved templates, various metal oxides could be applied as highly crystalline coatings with high structural regularity of the mesopores (spherical, size larger than 12 nm).^[34–36]

Beside the technically highly relevant anatase, ZrO_2 , CeO_2 , and a variety of mixed intermediary ternary oxide

mixtures of the two metals have also been synthesized (see Figure 8).^[34]

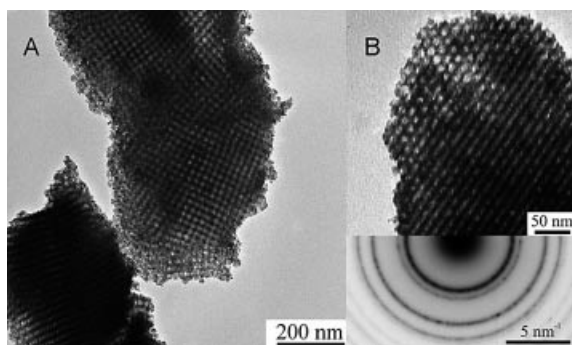


Figure 8. Crystalline, mesoporous CeO_2 films prepared from molecular precursors (A),^[34b] and mesoporous powder obtained from preformed CeO_2 nanoparticles (B).^[16a] The selected-area electron diffraction pattern (bottom part of B) proves the crystallinity of the mesopore walls.

Those ceria/zirconia systems are interesting for various applications. Compared to other metal oxides, ceria and zirconia are chemically and thermally extraordinarily stable and are therefore used as catalyst supports and in ceramic membranes for sensing and catalysis. Ceria has just one polymorph (fluorite structure), and can switch easily between Ce^{4+} and Ce^{3+} , balancing the charge difference with oxygen vacancies. This distinct property makes cerium oxide in the form of mesoporous layers an interesting candidate for solid-oxide fuel cells.

Porous crystalline films with very high thermal stability and related crystallization temperatures, such as Al_2O_3 ^[35a] and HfO_2 ,^[35b] have also been made. The case studies on HfO_2 had the advantage that removal of the template and crystallization are thermally clearly separate processes. Here, it could be demonstrated that the transformation of the initial self-assembled composite, consisting of the block copolymer and weakly condensed metal oxyhydrates, into the final mesoporous, crystalline metal oxide proceeds through the steps of inorganic condensation, template removal, and final crystallization. WAXS/SAXS experiments performed in situ during the heat treatment revealed that the crystallization has to be adjusted to be a solid–solid transformation from an almost completely dry, water-free, amorphous metal oxide into its crystalline counterpart. It is essential that the BC template is stable enough to support the mesostructure up to a temperature (350–400 °C under nitrogen) where the anhydrous and amorphous condensed metal oxide species is formed.

As shown for Al_2O_3 , a slightly higher structural size is also favorable for the mechanical stability of the intermediary amorphous thin pore walls and the final thermal stability. Well organized $\gamma\text{-Al}_2\text{O}_3$ films were only accessible when the pore size was increased to about 20 nm^[35a] (Figure 9).

Furthermore, even such complex materials as perovskites (e.g. BaTiO_3 , SrTiO_3 , and their substitution products) can now be obtained as mesoporous films,^[36] which is particu-

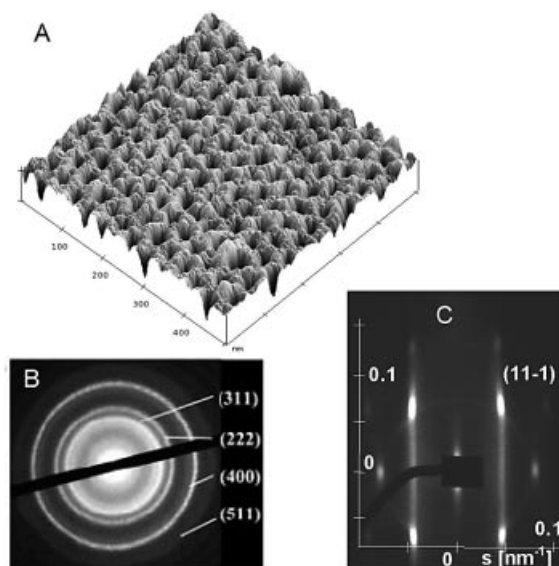


Figure 9. Crystalline, mesoporous films of $\gamma\text{-Al}_2\text{O}_3$, heat-treated at 900 °C.^[35a] A: Atomic force microscopy image. B: Selected-area electron diffraction, underlining the polycrystalline character. C: 2D SAXS pattern obtained at a low angle of incidence with respect to the substrate, proving the close to perfect orientation of the mesostructure in the z -direction.

larly interesting for a number of reasons (Figure 10). First, such materials are more difficult to accomplish in the desired stoichiometric composition by ordinary sol–gel methods. Secondly, the class of perovskites is linked to properties such as ferroelectricity, piezoelectricity, adjustable bandgaps, or even high-temperature superconductivity.^[37]

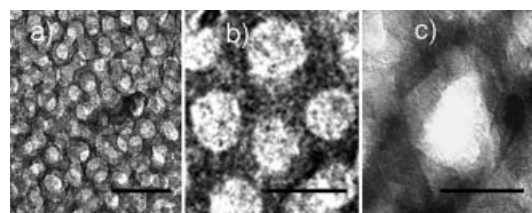


Figure 10. Structural changes in mesoporous SrTiO_3 perovskite films upon transformation from the amorphous (a and b) to the crystalline phase. The walls, in spite of the complex composition, are nevertheless homogeneous and single crystalline. Scale bars from left to right: 50 nm, 20 nm, and 10 nm.

For other oxide systems, such as Nb_2O_5 , a newly emerging dynamic effect sets in. On a mesoscopic scale, these films look quite similar to all the other previously described ones (Figure 11). Both WAXS and electron diffraction, however, show that the structure is built up by aligned single nanoparticles, that is, the nanoparticles “sense” their mutual organization and orient together in one energetically favorable direction.^[38] This effect also occurs for dense sol–gel films made by similar protocols and has been called “soft epitaxy”. It might become the basis for the generation of oriented films by simple chemical coating means.

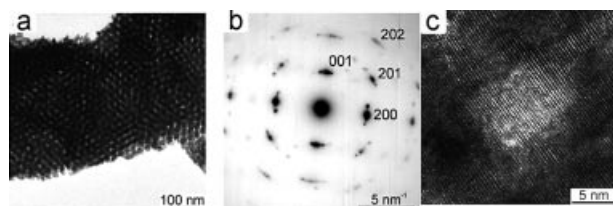


Figure 11. Soft epitaxy of mesoporous niobium oxide made by nanocasting: a) TEM of a porous film; b) electron diffraction of the same area, indicating an epitaxial alignment of the formed nanoparticles to the surface and each other; c) HRTEM of one single pore supporting the rather high degree of mutual organization.

The special functionality of crystalline oxide films has been explored both for SnO_2 ^[39] and WO_3 .^[40] In the case of SnO_2 , it was shown that the resulting porous thin-films are conducting, which is a prerequisite for their use as sensors and as electrodes. For WO_3 , reversible electrochromism, which is the reversible change of the transparency of those films with applied electric fields, has also been observed (Figure 12). The switching time in these films is much shorter than classical thin-films analogous to this structure (already applied in switchable rear mirrors) as electrons only have to be moved from the walls to the pore interior (Figure 12).

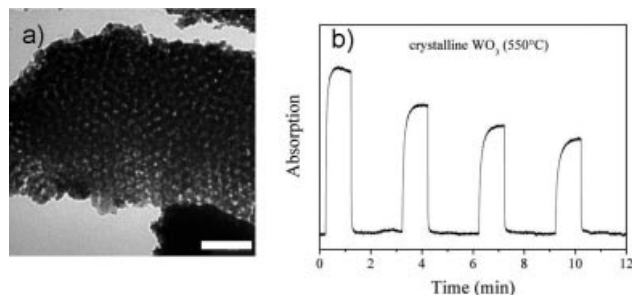


Figure 12. Mesoporous WO_3 (TEM, a) prepared with KLE block copolymers shows improved electrochromic switching. b) The absorption at 450 nm as a function of applied voltage. The mesoporous, crystalline mesostructure with its much higher surface area and short transport paths leads to a much faster coloration and decoloration than previous materials.

Very recently, some new approaches have been developed that extend nanocasting in a even more general frame and bypass some of the aforementioned problems. For instance, in the method of Holmes and Watkins the films are exposed to solutions of metal oxide precursors in supercritical CO_2 .^[41] This procedure has the advantage that capillary forces are absent and that the films have higher temperature stability because of the supercritical conditions. In separate work, Chmelka et al. first cross-linked the mesophases of block copolymers featuring additional double bonds,^[42] and then the inorganic precursor was infiltrated. This approach reduces the disruption of the BC mesophase upon condensation of the metal salts.

Wiesner and Gruner et al.^[43] have used extended amphiphilic dendrimers as templates, the self assembly of which is also expected to be rather robust against variations of the

environment. Another interesting approach was introduced by Domen:^[44] first, an amorphous mesoporous oxide is prepared, which is then followed by carbon deposition inside the pores, which acts as a temperature-stable scaffold. The material is then crystallized at elevated temperature, where the carbon prevents mesostructural collapse. Finally, the carbon is oxidized by calcination in oxygen to generate the pure inorganic scaffold.

4. Mesoporous Metals and Other Semiconductors

Aside from mesoporous metal oxides, mesoporous elemental metals, e.g. Pt, Pd, and Ni, have also been obtained by block copolymer templating. In principle, mesoporous metals are also accessible through the schematic principle depicted in Figure 1. Similar to mesoporous oxides, in the first step, reducible metal salts (PdCl_2 , H_2PtCl_6 , etc.) are distributed around the block copolymer domains. The preparation of the corresponding metals is more delicate because of the additional reduction step, which can be performed by electrodeposition (for instance on gold electrodes) or chemically, for example with metallic Zn. A second problem of these strategies is the high densification of matter throughout metal formation.

The Attard group has reported the electrochemical preparation of mesoporous metal electrodes (Figure 13, A),^[45] which could be interesting for various applications such as fuel cells (Ni) or electrochemical hydrogenation of organic species (Pd, Pt). Yamauchi et al.^[46] have described the generation of mesostructured particles of Ni (Figure 13) and Ni-Co alloys, partly by electrodeless methods, especially by using organic reducing agents such as dimethylaminoborane or sodium borohydride. Furthermore, Kucernak has demonstrated that it is possible to obtain mesostructures of otherwise inaccessible mesoporous “alloys” such as Pt/Ru.^[47] Such two-phase, mesostructured metal blends show high promise for catalytic applications, such as in fuel cells.

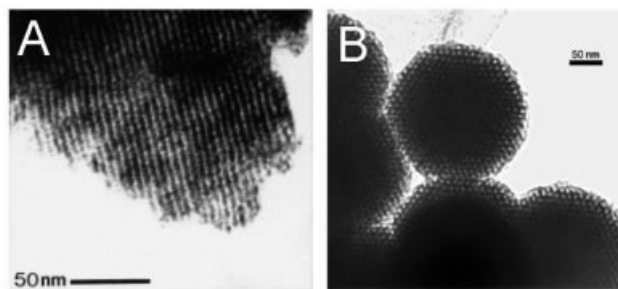


Figure 13. Mesoporous Pt^[45a] (A) and mesoporous Ni^[46a] particles (B).

Using oligomeric nonionic surfactants, even non-oxidic semiconductors have been made. Stupp et al.^[48] have been able to mesostructure thin films of CdS, CdSe, and ZnS, while for Ag_2S , CuS, HgS, and PbS the same methodology only resulted in compound films without mesoscopic features. Nandhakumar et al.^[49] have extended this approach

to synthesize mesostructured CdTe films with excellent optical properties. As these experiments were already possible with rather short oligomeric structures, it is expected that the advantages of block copolymer templates can also be transferred to these classes of inorganic materials.

Conclusion and Outlook

Nanocasting with block copolymer templates has turned into a powerful instrument for generating inorganic materials with mesostructure, porosity, and a high surface area, as documented by the broad variety of new materials described above. In nanocasting, the self-assembly of “soft”, fragile matter is literally hard-copied into inorganic hard matter, with all the advantageous properties resulting from the inorganic world. Through the hard-copy approach, the inorganic films are fitted out with the properties that make them valuable for different areas of materials science, e.g. chemical sensing, piezoelectricity, catalysis, electrochromism, solar cells, light-emitting diodes, etc. All these applications benefit from an optimized mesostructure, conduction pathways, or addressed binary interface contacts.

It is our personal view that these new materials are the first case where self-assembly will have a significant impact on nanosciences, especially for diverse electrochemical applications where complex metal oxides are needed with high surface areas. It is also very likely that various fields such as electrochromism, batteries, and electrode materials will benefit dramatically from progress in the preparation of mesoporous inorganic materials and metals. However, there are still some important challenges that hinder a broader application of block copolymer templated mesostructures in technical devices. For instance, for catalysis and electrodes it would be desirable to prepare crystalline, mesoporous metal oxides in the form of macroscopic monoliths, which can also be obtained in arbitrary shapes. Moreover, although various mesostructures have been obtained as high quality thin films with thicknesses of up to several micrometers, the preparation of much thicker layers is still a problem. Such geometries are, however, needed for various applications, for example for catalytically active coatings.

Another point of exploration and interest are hierarchical mesostructures with their expectedly superior transport properties, because larger pores could serve as transport pores, reduce back-pressure, and enhance diffusion. Such hierarchical structures could, in principle, be obtained by mixing the corresponding block copolymer micelles of different sizes. However, this build-up of hierarchically arranged micelles is not a trivial task because block copolymers tend to form either mixed micelles or phase-separate macroscopically.^[50,51]

Furthermore, new types of block copolymer could open up a new chapter in templating. So far, self-assembly has mainly been carried out in close-to-aqueous systems. If templates were available that form self-organized lyotropic structures in a variety of solvents, this would dramatically facilitate processing and allow broader synthetic access to

other porous materials, in particular for substances which are sensitive to water.

Evidently, in spite of the huge progress in the field of block copolymer self-assembly, there are still fascinating new opportunities for inorganic and materials chemistry, which will, in our opinion, keep this area very active for the next few years.

- [1] a) G. S. Attard, J. G. Glyde, C. G. Goltner, *Nature* **1995**, 378, 366–368; b) G. S. Attard, C. G. Goltner, J. M. Corker, S. Henke, R. H. Templer, *Angew. Chem.* **1997**, 109, 1372–1374; *Angew. Chem. Int. Ed. Engl.* **1997**, 36, 1315.
- [2] a) C. G. Goltner, S. Henke, M. C. Weissenberger, M. Antonietti, *Angew. Chem.* **1998**, 110, 633–636; *Angew. Chem. Int. Ed.* **1998**, 37, 613; b) C. G. Goltner, M. Antonietti, *Adv. Mater.* **1997**, 9, 431; c) M. C. Weissenberger, C. G. Goltner, M. Antonietti, *Ber. Bunsen-Ges. Phys. Chem.* **1997**, 101, 1679–1682.
- [3] S. Polarz, M. Antonietti, *Chem. Commun.* **2002**, 2593–2604.
- [4] U. Ciesla, F. Schuth, *Microporous Mesoporous Mater.* **1999**, 27, 131–149.
- [5] a) F. S. Bates, G. H. Fredrickson, *Annu. Rev. Phys. Chem.* **1990**, 41, 525–557; b) I. W. Hamley, *Philos. Trans. R. Soc. London, A* **2001**, 359, 1017–1044.
- [6] a) C. G. Goltner, B. Berton, E. Kramer, M. Antonietti, *Adv. Mater.* **1999**, 11, 395–398; b) S. Forster, B. Berton, H. P. Hentze, E. Kramer, M. Antonietti, P. Lindner, *Macromolecules* **2001**, 34, 4610–4623; c) H. P. Hentze, E. Kramer, B. Berton, S. Forster, M. Antonietti, M. Dreja, *Macromolecules* **1999**, 32, 5803–5809.
- [7] a) D. Zhao, Q. Huo, J. Feng, B. F. Chmelka, G. D. Stucky, *J. Am. Chem. Soc.* **1998**, 120, 6024–6036; b) D. Zhao, J. Feng, Q. Huo, N. Melosh, G. H. Fredrickson, B. F. Chmelka, G. D. Stucky, *Science* **1998**, 279, 548–552.
- [8] E. Kramer, S. Forster, C. Goltner, M. Antonietti, *Langmuir* **1998**, 14, 2027–2031.
- [9] a) A. Thomas, H. Schlaad, B. Smarsly, M. Antonietti, *Langmuir* **2003**, 19, 4455–4459; b) M. Groenewolt, M. Antonietti, S. Polarz, *Langmuir* **2004**, 20, 7811–7819; c) C. G. Goltner, B. Berton, E. Krämer, M. Antonietti, *Chem. Commun.* **1998**, 2287–2288.
- [10] M. Templin, A. Franck, A. DuChesne, H. Leist, Y. M. Zhang, R. Ulrich, V. Schädler, U. Wiesner, *Science* **1997**, 278, 1795–1798.
- [11] H. P. Hentze, E. Krämer, B. Berton, S. Forster, M. Antonietti, *Macromolecules* **1999**, 32, 5803–5809.
- [12] C. J. Brinker, Y. F. Lu, A. Sellinger, H. Y. Fan, *Adv. Mater.* **1999**, 11, 579–585.
- [13] a) W. Ruland, B. Smarsly, *J. Appl. Crystallogr.* **2004**, 37, 575–684; b) W. Ruland, B. Smarsly, *J. Appl. Crystallogr.* **2005**, 38, 78–86.
- [14] A. Gibaud, D. Grosso, B. Smarsly, A. Baptiste, J. F. Bardeau, F. Babonneau, D. A. Doshi, Z. Chen, C. J. Brinker, C. Sanchez, *J. Phys. Chem. B* **2003**, 107, 6114–6118.
- [15] F. Bosc, A. Ayral, P. A. Albouy, C. Guizard, *Chem. Mater.* **2003**, 15, 2463–2468.
- [16] a) A. S. Desphande, N. Pinna, B. Smarsly, M. Antonietti, M. Niederberger, *Small* **2005**, 1, 313–316; b) J. Ba, J. Polleux, M. Antonietti, M. Niederberger, *Adv. Mater.* **2005**, DOI 10.1002/adma.200501018.
- [17] a) N. Pinna, G. Garnweitner, M. Antonietti, M. Niederberger, *J. Am. Chem. Soc.* **2005**, 127, 5608–5612; b) N. Pinna, G. Garnweitner, M. Antonietti, M. Niederberger, *Adv. Mater.* **2004**, 16, 2196–2200; c) M. Niederberger, M. H. Bard, G. D. Stucky, *J. Am. Chem. Soc.* **2002**, 124, 13642–13643.
- [18] B. Smarsly, S. Polarz, M. Antonietti, *J. Phys. Chem. B* **2001**, 105, 10473–10483.
- [19] C. G. Goltner, B. Smarsly, B. Berton, M. Antonietti, *Chem. Mater.* **2001**, 13, 1617–1624.

- [20] a) M. Jaroniec, M. Kruk, C. H. Ko, R. Ryoo, *Chem. Mater.* **2000**, *12*, 1961–1968; b) R. Ryoo, C. H. Ko, M. Kruk, V. Antochshuk, M. Jaroniec, *J. Phys. Chem. B* **2000**, *104*, 11465.
- [21] B. Smarsly, M. Thommes, P. I. Ravikovitch, A. V. Neimark, *Adsorption* **2005**, *11*, 653–655.
- [22] M. Impéror-Clerc, P. Davidson, A. Davidson, *J. Am. Chem. Soc.* **2000**, *122*, 11925–11933.
- [23] B. Smarsly, C. G. Goltner, M. Antonietti, W. Ruland, E. Hönkisch, *J. Phys. Chem. B* **2001**, *105*, 831–840.
- [24] a) A. Galarneau, N. Cambon, F. Di Renzo, R. Ryoo, M. Choi, F. Fajula, *New J. Chem.* **2003**, *27*, 73–79; b) B. L. Newalkar, S. Komarneni, *Chem. Mater.* **2001**, *13*, 4573–4579; c) K. Miyazawa, S. Inagaki, *Chem. Commun.* **2000**, 2121–2122.
- [25] M. Grätzel, *Nature* **2001**, *414*, 338–344.
- [26] I. Mora-Seró, *J. Phys. Chem. B* **2005**, *109*, 3371–3380.
- [27] D. M. Antonelli, J. Y. Ying, *Curr. Opin. Colloid Interf. Sci.* **1996**, *1*, 523–529.
- [28] P. D. Yang, T. Deng, D. Y. Zhao, P. Y. Feng, D. Pine, B. F. Chmelka, G. M. Whitesides, G. D. Stucky, *Science* **1998**, *282*, 2244.
- [29] a) O. Dag, I. Soten, O. Celik, S. Polarz, N. Coombs, G. A. Ozin, *Adv. Funct. Mater.* **2003**, *13*, 30–36; b) S. Y. Choi, M. Mamak, N. Coombs, N. Chopra, G. A. Ozin, *Adv. Funct. Mater.* **2004**, *14*, 335–344; c) S. Y. Choi, M. Mamak, S. Speakman, N. Chopra, G. A. Ozin, *Small* **2005**, *1*, 226–232.
- [30] a) D. Grosso, G. Soler-Illia, F. Babonneau, C. Sanchez, P. A. Albouy, A. Brunet-Bruneau, A. R. Balkenende, *Adv. Mater.* **2001**, *13*, 1085; b) E. L. Crepaldi, G. Soler-Illia, D. Grosso, C. Sanchez, *New J. Chem.* **2003**, *27*, 9–13; c) D. Grosso, G. J. D. A. Soler-Illia, E. L. Crepaldi, F. Cagnol, C. Sinturel, A. Bourgeois, A. Brunet-Bruneau, H. Amenitsch, P. A. Albouy, C. Sanchez, *Chem. Mater.* **2003**, *15*, 4562–4570; d) E. L. Crepaldi, G. J. de A. A. Soler-Illia, D. Grosso, F. Cagnol, F. Ribot, C. Sanchez, *J. Am. Chem. Soc.* **2003**, *125*, 9770–9786; e) D. O. de Zárate, C. Boissière, D. Grosso, P. A. Albouy, H. Amenitsch, P. Amoros, C. Sanchez, *New J. Chem.* **2005**, *29*, 141–144; f) P. C. Angelomé, S. Aldabe-Bilmes, M. E. Calvo, E. L. Crepaldi, D. Grosso, C. Sanchez, G. J. A. A. Soler-Illia, *New J. Chem.* **2005**, *29*, 59–63.
- [31] a) M. Groenewolt, T. Brezesinski, H. Schlaad, M. Antonietti, P. W. Groh, B. Ivan, *Adv. Mater.* **2005**, *17*, 1158; b) B. Smarsly, D. Grosso, T. Brezesinski, N. Pinna, C. Boissière, M. Antonietti, C. Sanchez, *Chem. Mater.* **2004**, *16*, 2948–2952.
- [32] H. Schlaad, T. Krasia, M. Antonietti, *J. Am. Chem. Soc.* **2004**, *126*, 11307–11310.
- [33] a) M. Antonietti, S. Forster, J. Hartmann, S. Oestreich, *Macromolecules* **1996**, *29*, 3800–3806; b) M. Antonietti, S. Forster, S. Oestreich, *Macromol. Symp.* **1997**, *121*, 75–88; c) S. Klingelhofer, W. Heitz, A. Greiner, S. Oestreich, S. Forster, M. Antonietti, *J. Am. Chem. Soc.* **1997**, *119*, 10116–10120.
- [34] a) T. Brezesinski, M. Groenewolt, N. Pinna, M. Antonietti, B. Smarsly, *New J. Chem.* **2005**, *29*, 237–242; b) T. Brezesinski, C. Erpen, K. I. Iimura, B. Smarsly, *Chem. Mater.* **2005**, *17*, 1683–1690.
- [35] a) M. Kuemmel, D. Grosso, C. Boissière, B. Smarsly, T. Brezesinski, P. A. Albouy, H. Amenitsch, C. Sanchez, *Angew. Chem. Int. Ed.* **2005**, *44*, 4589–4592; b) T. Brezesinski, B. Smarsly, K. I. Iimura, D. Grosso, C. Boissière, H. Amenitsch, M. Antonietti, C. Sanchez, *Small* **2005**, *1*, 889–898.
- [36] D. Grosso, C. Boissière, B. Smarsly, T. Brezesinski, N. Pinna, P. A. Albouy, H. Amenitsch, M. Antonietti, C. Sanchez, *Nat. Mater.* **2004**, *3*, 787–792.
- [37] a) A. S. Balla, R. Guo, R. Roy, *Mat. Res. Innovat.* **2000**, *4*, 3–26; b) C. D. Chandler, C. Roger, M. J. Hampden-Smith, *Chem. Rev.* **1993**, *93*, 1205–1241.
- [38] B. Smarsly, T. Brezesinski, M. Groenewolt, N. Pinna, H. Amenitsch, M. Antonietti, *Nat. Mater.*, manuscript submitted.
- [39] T. Brezesinski, B. Smarsly, A. Fischer, M. Groenewolt, D. Grosso, C. Sanchez, M. Antonietti, *Adv. Funct. Mater.*, manuscript submitted.
- [40] T. Brezesinski, D. Fattakhova Rohlfing, S. Sallard, M. Antonietti, B. M. Smarsly, *J. Am. Chem. Soc.*, manuscript submitted.
- [41] a) K. X. Wang, B. D. Yao, M. A. Morris, J. D. Holmes, *Chem. Mater.* **2005**, *17*, 4825–4831; b) R. A. Pai, R. Humayun, M. T. Schulberg, A. Sengupta, J. N. Sun, J. J. Watkins, *Science* **2004**, *303*, 507–510.
- [42] R. C. Hayward, B. F. Chmelka, E. J. Kramer, *Macromolecules* **2005**, *38*, 7768–7783.
- [43] B. K. Cho, A. Jain, S. Mahajan, H. Ow, S. M. Gruner, U. Wiesner, *J. Am. Chem. Soc.* **2004**, *126*, 4070–4071.
- [44] J. N. Kondo, T. Katou, D. Lu, M. Hara, K. Domen, *Stud. Surf. Sci. Cat.* **2004**, *154*, 951–957.
- [45] a) G. S. Attard, P. N. Bartlett, N. R. B. Coleman, J. M. Elliott, J. R. Owen, J. H. Wang, *Science* **1997**, *278*, 838–840; b) P. A. Nelson, J. M. Elliott, G. S. Attard, J. R. Owen, *Chem. Mater.* **2002**, *14*, 524–529; c) J. M. Elliott, G. S. Attard, P. N. Bartlett, N. R. B. Coleman, D. A. S. Merckel, J. R. Owen, *Chem. Mater.* **1999**, *11*, 3602–3609.
- [46] a) Y. Yamauchi, T. Momma, T. Yokoshima, K. Kuroda, T. Osaka, *J. Mater. Chem.* **2005**, *15*, 1987–1994; b) Y. Yamauchi, T. Yokoshima, T. Momma, T. Osaka, K. Kuroda, *J. Mater. Chem.* **2004**, *14*, 2935–2940; c) Y. Yamauchi, T. Yokoshima, T. Momma, T. Osaka, K. Kuroda, *Chem. Lett.* **2004**, *33*, 1576–1579; d) Y. Yamauchi, T. Yokoshima, H. Mukaibo, M. Tezuka, T. Shigeno, T. Momma, T. Osaka, K. Kuroda, *Chem. Lett.* **2004**, *33*, 543.
- [47] a) J. Jiang, A. Kucernak, *Chem. Mater.* **2004**, *16*, 1362–1367; b) J. Jiang, A. Kucernak, *J. Electroanal. Chem.* **2003**, *543*, 187–199.
- [48] P. V. Braun, P. Osenar, V. Tohver, S. B. Kennedy, S. I. Stupp, *J. Am. Chem. Soc.* **1999**, *121*, 7302–7309.
- [49] I. S. Nandhakumar, T. Gabriel, X. Li, G. S. Attard, M. Markham, D. C. Smith, J. J. Baumberg, *Chem. Commun.* **2004**, *12*, 1374–1375.
- [50] T. Sen, G. J. T. Tiddy, J. L. Casci, M. W. Anderson, *Angew. Chem. Int. Ed.* **2003**, *42*, 4649–4653.
- [51] D. B. Kuang, T. Brezesinski, B. Smarsly, *J. Am. Chem. Soc.* **2004**, *126*, 10534–10535.

Received: November 10, 2005

Published Online: February 21, 2006